



Risk Factors, Hyaluronidase Expression, and Clinical Immunogenicity of Recombinant Human Hyaluronidase PH20, an Enzyme Enabling Subcutaneous Drug Administration

Marie A. Printz¹ · Barry J. Sugarman² · Rudolph D. Paladini² · Michael C. Jorge² · Yan Wang¹ · David W. Kang¹ · Daniel C. Maneval² · Michael J. LaBarre¹

Received: 30 June 2022 / Accepted: 23 September 2022 / Published online: 20 October 2022
© The Author(s) 2022

Abstract

Multiple FDA-approved and clinical-development stage therapeutics include recombinant human hyaluronidase PH20 (rHuPH20) to facilitate subcutaneous administration. As rHuPH20-reactive antibodies potentially interact with endogenous PH20, we investigated rHuPH20 immunogenicity risk through hyaluronidase tissue expression, predicted B cell epitopes, CD4+ T cell stimulation indices and related these to observed clinical immunogenicity profiles from 18 clinical studies. Endogenous hyaluronidase PH20 expression in humans/mice was assessed by reverse transcriptase-polymerase chain reaction (RT-PCR), quantitative RT-PCR, and deep RNA-Seq. rHuPH20 potential T cell epitopes were evaluated *in silico* and confirmed *in vitro*. Potential B cell epitopes were predicted for rHuPH20 sequence *in silico*, and binding of polyclonal antibodies from various species tested on a rHuPH20 peptide microarray. Clinical immunogenicity data were collected from 2643 subjects. From 57 human adult and fetal tissues previously screened by RT-PCR, 22 tissue types were analyzed by deep RNA-Seq. Hyaluronidase PH20 messenger RNA expression was detected in adult human testes. *In silico* analyses of the rHuPH20 sequence revealed nine T cell epitope clusters with immunogenic potential, one cluster was homologous to human leukocyte antigen. rHuPH20 induced T cell activation in 6–10% of peripheral blood mononuclear cell donors. Fifteen epitopes in the rHuPH20 sequence had the potential to cross-react with B cells. The cumulative treatment-induced incidence of anti-rHuPH20 antibodies across clinical studies was 8.8%. Hyaluronidase PH20 expression occurs primarily in adult testes. Low CD4+ T cell activation and B cell cross-reactivity by rHuPH20 suggest weak rHuPH20 immunogenicity potential. Restricted expression patterns of endogenous PH20 indicate low immunogenicity risk of subcutaneous rHuPH20.

Keywords Hyaluronidase · rHuPH20-reactive antibodies · Immunogenicity · Endogenous PH20

Introduction

Human hyaluronidases are a family of enzymes, hyaluronidase 1 (HYAL1), HYAL2, HYAL3, HYAL4, hyaluronidase PH20 (Sperm Adhesion Molecule 1 [SPAM1] gene product), and the pseudogene hyaluronoglucosaminidase pseudogene 6 (*HYALP6*, formerly classified as *HYALP1*). Hyaluronidases depolymerize hyaluronan (HA), a naturally occurring glycosaminoglycan and component of the

extracellular matrix (1–5). Each hyaluronidase enzyme has a unique tissue distribution. Hyaluronidase PH20 is primarily expressed in mammalian testis and the epididymis (6, 7). However, various laboratories have reported hyaluronidase PH20 expression in human cartilage (8), breast tissue (9), the murine kidney (10), endometrium (11), oligodendrocyte progenitor cells (12), and the corpus callosum (13). The claim of hyaluronidase PH20 expression in the corpus callosum of the murine brain and oligodendrocyte precursor cells could have important implications, prompting us to better understand the endogenous expression of hyaluronidases in these and other tissues.

A recombinant soluble human hyaluronidase PH20 (rHuPH20) enzyme was derived from its endogenous counterpart, hyaluronidase PH20, differing only in the absence of the carboxy terminal putative glycosylphosphatidylinositol

✉ Marie A. Printz
publications@halozyme.com

¹ Halozyme Therapeutics, Inc., 11388 Sorrento Valley Rd, San Diego, California 92121, USA

² Formerly with Halozyme Therapeutics, Inc., San Diego, California, USA



anchor present in endogenous enzyme (14). rHuPH20 was approved by the US Food and Drug Administration in 2005 for use in subcutaneous (SC) fluid administration for achieving hydration, to increase the dispersion and absorption of other injected drugs, and in SC urography for improving resorption of radiopaque agents (HYLENEX™) (15). As of May 2022, rHuPH20 has also been approved in more than 100 countries since 2013 as a co-formulated component or sequentially administered agent to facilitate the SC delivery of therapeutic molecules (16).

Recombinant proteins have the potential for inducing immunogenicity. Immune responses to therapeutic proteins can generate therapeutic-reactive antibodies by T cell-dependent or T cell-independent pathways (17). Therapeutic-reactive antibodies generated in response to recombinant proteins with endogenous counterparts can cause severe side effects by binding to the endogenous counterpart, with or without neutralization (18–20). Due to the high homology of rHuPH20 to human hyaluronidase PH20 (100%, minus the C-terminal truncation) (21) and more limited homology to other human hyaluronidases (33–42%) (22), rHuPH20-reactive antibodies could potentially bind endogenous hyaluronidase PH20, with or without neutralization. Pre-existing rHuPH20-reactive antibodies are present in 3–13% of people despite lack of exposure to rHuPH20 (21, 23, 24). Across clinical trials, the incidences of treatment-emergent rHuPH20-reactive antibodies remain low even after long-term exposure to rHuPH20 (21). Given the potential for cross-reactivity, an understanding of tissue expression levels of hyaluronidases is important to evaluate the immunogenic risk of rHuPH20.

Male mice lacking PH20 (PH20^{-/-}) are fertile, suggesting that hyaluronidase PH20 is not essential for fertilization. However, sperm of PH20^{-/-} mice shows a delayed dispersal of cumulus cells from the cumulus mass *in vitro*, resulting in delayed fertilization solely at the early stages post-insemination (25). While loss of either SPAM1 or HYAL5 alone does not cause male infertility in mice (26), studies with double knockout mice led the investigators to conclude that HYAL deficiency in sperm may be a significant risk factor for male sterility (26). Since hyaluronidase PH20 expression is well documented in adult testis and epididymis (6, 7, 27), the potential impact of rHuPH20-reactive antibodies on fertility is important to consider (28). Preclinical studies in mice (29), rabbits (30), sheep (31), and cynomolgus monkeys (32) indicate that the presence of neutralizing antibodies to hyaluronidase PH20 do not impair fertility and are not associated with adverse effects on pregnancy (30, 33), perhaps in part due to the structural aspects of immune privilege in the testis (34) and the limited access of plasma antibodies to sperm (35).

In a clinical survey study of 896 healthy volunteers (767 adults), approximately 5% (1/20) of the adult population tested positive for rHuPH20-reactive antibodies without

prior exposure to rHuPH20. rHuPH20-reactive antibody prevalence increased with age and was higher in males compared with females (23). Although the root cause for this baseline prevalence of rHuPH20-reactive antibodies remains unknown, no evidence of negative effects on fertility in rHuPH20-reactive antibody-positive women or men was seen (23).

Here, we assessed the endogenous expression of hyaluronidases in a variety of tissues using reverse transcriptase-polymerase chain reaction (RT-PCR), RT-quantitative PCR (qPCR), and transcriptome assessment via deep RNA-Seq, and evaluated the potential risk for rHuPH20-reactive antibodies to cross-react with B cell epitopes or elicit CD4+ T cell stimulation *in silico* and *in vitro*.

Methods

Tissues and Primary Cells

Corpus callosum, cortex, and testis tissues were isolated from adult male C57BL/6, NU/NU, and SCID mice (Charles River Laboratories, Wilmington, MA, USA). Mice were maintained in accordance with the Institutional Animal Care and Use Committee (IACUC) guidelines and experimental procedures conducted under approved IACUC protocols. Commercially available human primary oligodendrocyte precursors, neurons and astrocytes, and murine primary astrocytes and primary cortical neurons were obtained from ScienCell Research Laboratories, Inc. (Carlsbad, CA, USA).

Peripheral Blood Mononuclear Cell Isolation

Buffy coats from 50 healthy donors were obtained from the UK National Blood Transfusion Service (Addenbrooke's Hospital, Cambridge, UK), according to approval by the Addenbrooke's Hospital Local Research Ethics Committee. Peripheral blood mononuclear cells (PBMCs) were isolated from buffy coats by Lymphoprep™ (Axis-Shield Diagnostics Ltd, Dundee, UK) density centrifugation and CD8+ T cells were depleted using CD8+ RosetteSep™ (STEMCELL Technologies, Inc., London, UK). Donors were characterized by identifying human leukocyte antigen-DR isotype (HLA-DR) haplotypes using an HLA Sequence Specific Primer-PCR based tissue-typing kit (Biotest, Solihull, UK).

Primary Culture of Mouse Oligodendrocyte Precursor Cells

Mouse embryo cortex E14 neurospheres (STEMCELL Technologies, Inc., Cambridge, MA, USA) were cultured in NeuroCult™ basal medium (STEMCELL Technologies, Inc., Cambridge, MA, USA), supplemented with 20 ng/mL

of epidermal growth factor and basic fibroblast growth factor (both from PeproTech, Inc., Rocky Hill, NJ, USA). After expansion, oligodendrocyte precursor cell medium was added to the neurospheres to promote differentiation and approximately 1×10^6 cells were isolated for RNA extraction.

RNA Samples

Commercially available total RNA from a battery of human tissues was purchased from BioChain Institute, Inc., Newark, CA, USA; Ambion, Inc., Austin, TX, USA; US Biological Life Sciences, Salem, MA, USA; and Clontech Laboratories, Inc., Mountain View, CA, USA. Total RNA was isolated from human primary cell cultures and from the corpus callosum, cortex, and testis samples from C57BL/6, NU/NU, and SCID mice using TRIzol reagent (Ambion Life Technologies, Grand Island, NY, USA). Tissues were homogenized using the IKA Ultra Turrax (Cole-Parmer, Vernon Hills, IL, USA) and FastPrep 24 (MP Biomedicals, Santa Ana, CA, USA) according to manufacturer's instructions. After homogenization, 0.2 mL of chloroform was added to each sample and incubated (room temperature, 3 min).

Samples were clarified by centrifugation at 12,000 *g* for 15 min at 4°C. The aqueous phase was isolated, and 0.5 mL of 100% isopropanol added. Following incubation (10 min, room temperature), samples were centrifuged at 12,000 *g* (10 min, 4°C). Pellets were washed, air dried, and resuspended in DNA-suspension buffer with 5 µL of DNase I (RNase-free, 10 U) and 10X DNase I buffer and incubated (2 h, 37°C). Isolated RNA was treated with 10 U RNase-free DNase I (New England Biolabs, Ipswich, MA, USA) and purified using the RNeasy MinElute Cleanup Kit (Qiagen, Germantown, MD, USA) per manufacturer's instruction. RNA purity and quality were determined using a NanoDrop spectrophotometer (ThermoFisher-Scientific, Waltham, MA, USA) and RNA Integrity Number (RIN) values obtained with the 2100 Bioanalyzer system (Agilent Technologies, Inc., Santa Clara, CA, USA).

RNA was manually extracted from cultured, commercially available human neuronal cells, astrocytes, and oligodendrocyte precursors cells obtained from ScienCell (Carlsbad, CA, USA).

Complementary DNA Generation

Complementary DNA (cDNA) was generated using the SuperScript™ III First-Strand Synthesis System for RT-PCR (Invitrogen™, Carlsbad, CA, USA). In each cDNA sample, 1 µg of total RNA was mixed with 1 µL 50 µM oligo(dT)20, 1 µL 10 mM dNTP mix, and RNase-free water to 10 µL, incubated for 5 min at 65°C, and cooled on ice. A cDNA synthesis mix containing 2 µL 10X RT buffer, 4 µL 25 mM MgCl₂, 2 µL 0.1 M DTT, 1 µL of RNaseOUT, and 1 µL

SuperScript III RT was added to each sample and the samples were incubated for 50 min at 50°C. The reaction was terminated by 5 min incubation at 85°C, the samples were cooled on ice, and then incubated with 1 µL RNaseH for 20 min at 37°C. The samples were stored at -20°C.

Polymerase Chain Reaction

Polymerase chain reactions were carried out on murine cDNA samples using the Mastercycler® (Eppendorf, Hauppauge, NY, USA), using 124, 440, or 588 base pair (bp) PH20-specific amplicons. Each individual PCR comprised of 1 µL forward primer (20 µM), 1 µL reverse primer (20 µM), 5 µL 10X Pfu buffer, 1 µL cDNA, 1 µL Pfu Turbo DNA Polymerase, 1 µL dNTP mixture (10 µM), and 40 µL of PCR certified water. The murine PH20 primers sequences are provided in Table SI (13); murine glyceraldehyde 3-phosphate dehydrogenase primers were used as controls.

Quantitative PCR

qPCR reactions on human and murine cDNA samples were carried out using the Applied Biosystems ViiA 7 Real-Time PCR System (Life Technologies, Carlsbad, CA, USA). Each reaction comprised of 1 µL specific primer/probe set, 10 µL 2X Taqman Fast Advanced Master Mix, 1 µL template cDNA, and 8 µL PCR-certified water. Hyaluronidase PH20, HYAL5, Nestin, beta-actin, doublecortin, neuronal nuclei, growth associated protein 43, and platelet-derived growth factor receptor alpha polypeptide primer/probe sets were used in the assays.

Samples were assayed in triplicate or duplicate using Applied Biosystems Microamp Fast Optical 96-well reaction plate (Life Technologies, Carlsbad, CA, USA). The qPCR conditions were as follows: the number of cycles in each qPCR reaction was 45 and each was preceded by a hold stage of 2 min at 50°C followed by 10 min at 95°C; each cycle consisted of 15 s at 95°C followed by 1 min at 60°C. All data were analyzed using the Applied Biosystems ViiA 7 RUO software version 1.1 (Life Technologies, Carlsbad, CA, USA).

Deep RNA-Seq Library Preparation, Sequencing, and Analysis

Total RNA concentrations were determined using the QuantiT RNA assay (Invitrogen, Carlsbad, CA, USA) and RNA quality was evaluated using either the TapeStation or 2100 Bioanalyzer (Agilent Technologies, Santa Clara, CA, USA). Human total RNA samples (at least 250 ng total RNA per sample) with a minimum RIN of 8 were used for library construction and sequencing.

Total RNA was purified and bound to oligo-dT magnetic beads (Illumina, San Diego, CA, USA; performed by Beckman Coulter Genomics, Danvers, MA, USA) to capture the polyadenylated RNA. RNA was converted into a cDNA library and suitability for high-throughput DNA sequencing for subsequent cluster generation determined using Illumina's TruSeq RNA Sample Prep Kit v2 (Illumina, San Diego, CA, USA; performed by Beckman Coulter Genomics, Danvers, MA, USA) in accordance with manufacturer's instructions. The messenger RNA (mRNA) was fragmented enzymatically prior to the first and second cDNA synthesis. Illumina adaptors were ligated after the cDNA was end-repaired. Once the samples were indexed, the adaptor-ligated cDNA was PCR-amplified using a program of 15 cycles, and then purified using AMPure XP (Beckman Coulter Genomics, Danvers, MA, USA).

Final libraries were sequenced on a HiSeq 2500 instrument (Illumina, San Diego, CA, USA) and multiplexed in sequencing lanes with index-compatible libraries which aimed for approximately 42 million reads per library. Sequencing performance met Illumina specifications. Cluster density, Q30 scores, passing filter percentage, and base intensity were evaluated by Beckman Coulter Genomics.

Following sequencing, the data were demultiplexed by index using Casava 1.8.2 (Illumina, San Diego, CA, USA). For further expression analysis, one forward and one reverse fastq file for each sample were used. Mapping was performed using TopHat v2.0.9 in conjunction with Bowtie v1.0.0. TopHat was provided with a transcriptome reference generated from the Ensembl release 74 assemblies. Cufflinks v2.1.1 was used to detect genes and transcripts that were expressed based upon sequence alignment by TopHat v2.0.9. Subsequently, Cuffdiff v2.1.1 was used to collect fragments per kilobase of exon and per million expression values.

HLA Binding Affinity Prediction

The rHuPH20 amino acid sequence was analyzed *in silico* using the EpiMatrix algorithm for T cell epitope identification (EpiMatrix system; EpiVax Inc., Providence, RI, USA). The protein was parsed into nine overlapping 9-mer frames and predicted against a panel of eight common Class II alleles, whose coverage spans 95% of the human population (EpiMatrix system; EpiVax Inc., Providence, RI, USA). EpiMatrix assessment scores ranged between -3 and +3, with scores >1.64 considered as positive hits. The EpiMatrix Protein Score was defined as the difference between the sum of the protein's positive EpiMatrix assessment scores and an expected score calculated based on the amino acid length. An EpiMatrix Protein Score >20 was indicative of significant immunogenic potential.

Regional immunogenicity was evaluated by screening the results of the EpiMatrix analysis to look for regions with unusually high densities of putative T cell epitopes. Significant EpiMatrix scores within these regions were aggregated and normalized to create an EpiMatrix Cluster Immunogenicity score, where positive scores indicate increased immunogenic potential and negative scores indicate a decreased immunogenic potential relative to a randomly generated sequence.

EpiScreen™ Analysis: Proliferation Assay

PBMC from each donor were adjusted to $2-3 \times 10^6$ PBMC/mL (proliferation cell stock), plated in a 96-well plate, and incubated with $5 \mu\text{M}$ of peptide (full-length protein or five 15-mer rHuPH20 peptides; Table SII) or control for a total of 6 days. On day 6, $0.75 \mu\text{Ci}$ [^3H]-Thymidine (PerkinElmer, Beaconsfield, UK) was added, and the cultures were incubated for 18 h before harvesting onto filter mats in a Tomtec Mach III cell harvester (Tomtec, Hamden, CT, USA). Bound radioactivity was counted on a Microplate Beta Counter (PerkinElmer, Beaconsfield, UK). All experiments were performed in sextuplicate.

In addition to the EpiScreen proliferation assay, rHuPH20 was assessed in a time course T cell proliferation assay and an interleukin (IL)-2 ELISpot assay, to ensure no format-specific bias.

EpiScreen Time Course T Cell Proliferation Assays

rHuPH20 was assessed in the EpiScreen (Abzena, Cambridge, UK) time course T cell proliferation assay for the capacity to induce CD4+ T cell responses. rHuPH20 was tested against PBMCs from a cohort of 50 healthy donors and T cell proliferation measured by [^3H]-Thymidine uptake. PBMCs from each donor were plated in a 24-well plate at $4-6 \times 10^6$ PBMC/mL and incubated with $16 \mu\text{g/mL}$ of peptide or control (KLH, humanized A33, or culture medium). Cultures were incubated at 37°C for 8 days, with cells taken on days 5, 6, 7, and 8. Thereafter, $0.75 \mu\text{Ci}$ [^3H]-Thymidine (PerkinElmer, Beaconsfield, UK) was added, and the cells were incubated for 18 h at 37°C before harvesting onto filter mats in a TomTec Mach III cell harvester. Bound radioactivity was counted in a 1450 Microbeta Wallac Trilux Liquid Scintillation Counter (PerkinElmer, Beaconsfield, UK).

Interleukin-2 ELISpot Assay

ELISpot plates (Millipore, Watford, UK) were coated overnight with IL-2 capture antibody (R&D Systems, Abingdon, UK), washed, and incubated overnight in blocking buffer (1% BSA in PBS). Cell density was adjusted to $4-6 \times 10^6$ PBMC/mL,

and 100 μL of cells incubated with full length rHuPH20, A33 (positive control), or buffer for 8 days. ELISpot plates were washed, incubated with biotinylated anti-mouse detection antibody (R&D Systems, Abingdon, UK) for 1.5 h at 37°C, followed by incubation with streptavidin-AP (R&D Systems, Abingdon, UK) for 30 min at room temperature. Plates were then incubated with BCIP/NBT substrate (R&D Systems, Abingdon, UK) for 30 min at room temperature. The wells were washed with distilled H_2O , dried, and scanned on an Immunoscan[®] Analyser (Cellular Technology Limited, Cleveland, OH, USA) and spots per well were determined using Immunoscan[®] software, Version 5.

B Cell Epitope Prediction

Potential linear B cell epitopes on the rHuPH20 enzyme sequence were identified by ProImmune REVEAL[™] B Cell Linear Epitope Prediction software (ProImmune, Inc., Sarasota, FL, USA) using algorithms to predict antigenicity (two algorithms), hydrophobicity (six algorithms), surface probability (one algorithm), chain flexibility (one algorithm), and secondary structure (based on a hidden Markov model). Potential antigenic epitopes for rHuPH20 were identified by employing a model of the 3D crystal structure of rHuPH20 (Halozyme Therapeutics, Inc., San Diego, CA, USA), which was based on the crystal structure of HYAL1 using amino acids 2–403 of rHuPH20 (38% sequence identity). Potential epitopes were identified on the basis of structure and solvent accessibility (Accelrys[®] Discovery Studio Visualizer; Accelrys, Inc.; carried out by ProImmune, Inc., Sarasota, FL, USA).

B Cell Epitope Mapping

A library of 15-mer microarray peptides, overlapping by 10 amino acids, was generated based on the rHuPH20 sequence using ProArray Ultra[™] technology (ProImmune, Inc., Sarasota, FL, USA). A total of 88 synthesized peptides were immobilized onto ProArray Ultra slides in eight identical sub-arrays, along with standard ProArray Ultra control features (Table SIII) in sextuplicate spots. Three affinity purified antibody preparations against rHuPH20 incubated on the array: an anti-rHuPH20 mouse monoclonal antibody immunoglobulin G1 (IgG1; clone 3E8), an anti-rHuPH20 rabbit polyclonal antibody, derived after hyperimmunization of rabbits with rHuPH20, and an rHuPH20-reactive human immunoglobulin G (IgG), purified from Gammagard[™] Liquid (human Ig infusion 10%; Takeda, Lexington, MA, USA).

The array slides were blocked and incubated with the antibody samples (0.5 ng/mL to 30 $\mu\text{g}/\text{mL}$) for 2 h. Antibody binding was detected with the appropriate fluorescently

labeled secondary antibody (anti-mouse IgG, anti-human IgG, or anti-rabbit IgG). As control, slides were incubated with labeled secondary antibody alone. Following several washing steps, the array slides were scanned using a high-resolution fluorescence scanner with appropriate wavelength settings and the resulting image processed and analyzed using Array-Pro Analyzer (Media Cybernetics, Inc., Rockville, Maryland, USA), showing the signal intensity as measurements for each peptide.

Results

Hyaluronidase PH20 Expression Is Localized to the Testis

The expression of human hyaluronidase genes in adult and fetal human tissue samples and in human primary cell cultures was analyzed using a deep RNA-Seq platform. Hyaluronidase PH20 mRNA was detected in the adult human testes, with steady-state levels peaking at fragments per kilobase per million reads values >15.8 (Fig. 1a). Notably, hyaluronidase PH20 mRNA was not detected in samples of neuronal origin including the brain, corpus callosum, oligodendrocyte precursors, astrocytes, and neurons, nor in other adult (kidney, placenta, prostate, skeletal muscle, skin, or synovium) or fetal (colon, kidney, ovary, pancreas, prostate, small intestine, or stomach) tissues.

In contrast, steady-state levels of HYAL1, HYAL2, and HYAL3 mRNAs were detected in a broad range of adult and fetal tissues, including the brain, bone, kidney, and colon, and in primary neuronal cell cultures. Steady-state levels of HYAL2 mRNA were highest in all tissue types compared with HYAL1 and HYAL3. HYAL4 mRNA expression was limited to adult bone, placenta, testes, and fetal ovary (Fig. 1a) tissue. Similarly, a directed query to the Allen Brain Atlas transcriptome database (Allen Institute, Washington, USA) (36) did not detect expression of hyaluronidase PH20 or HYAL4 expression in the human brain (Fig. 1b).

The expression of hyaluronidase PH20 in oligodendrocyte precursor, neuron, and astrocyte primary cell cultures was further analyzed in human and mouse samples. Hyaluronidase PH20 mRNA was not detected in human or mouse primary cell cultures using qPCR analysis but was observed in control adult testis samples (Fig. 2a). A similar pattern of gene expression was found by PCR analysis of cDNA from the corpus callosum, cortex, and testis of C57BI/6, NU/NU, and SCID mice. Amplicons corresponding to murine PH20-specific 124 bp, 440 bp, and 588 bp primer sets (13) were observed only in the testis samples and could not be detected in the cortex or corpus callosum from mice (Fig. 2b).

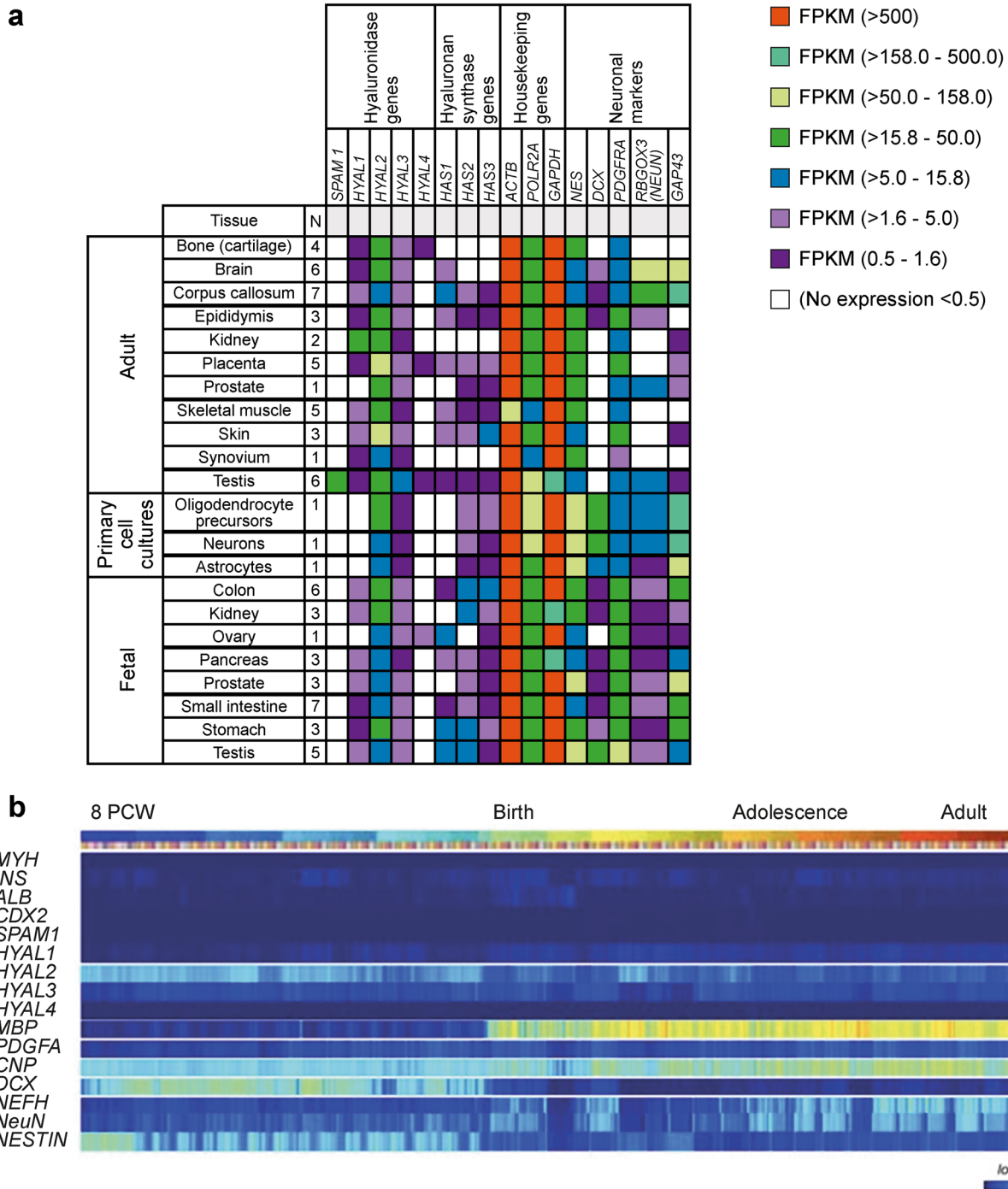
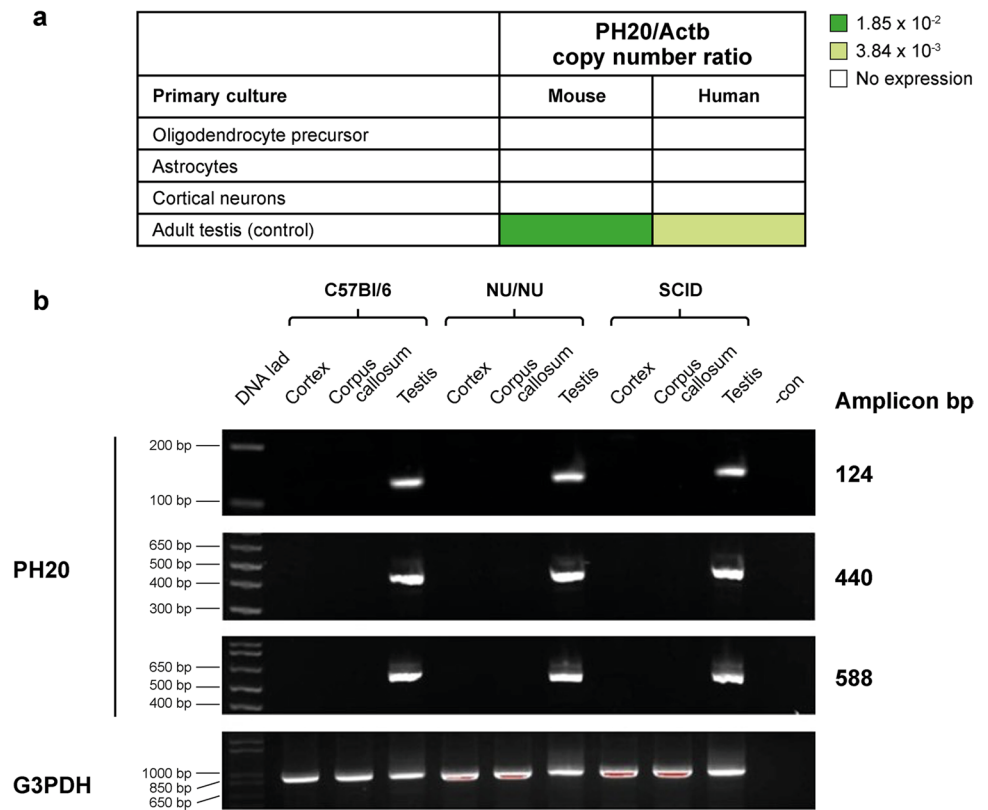


Fig. 1 Hyaluronidase expression pattern. **a** Heatmap depicting expression of hyaluronidase genes in human tissues and primary neuronal cell culture. **b** Allen Brain Atlas (36) query in heat map format, expression of human hyaluronidase across 13 developmental stages in 8–16 different brain structures. Actb, beta-actin; ALB, albumin; CDX2, caudal type homeobox 2; CNP, 2',3'-cyclic nucleotide 3' phosphodiesterase; DCX, doublecortin; FPKM, fragments per kilobase per million reads; GAP43, growth associated protein 43;

GAPDH, glyceraldehyde-3-phosphate dehydrogenase; HAS, hyaluronan synthase gene; HYAL, hyaluronoglucosaminidase; INS, insulin; MBP, myelin basic protein; MYH, myosin heavy chain; NEFH, neurofilament heavy chain; NES, nestin; NeuN, neuronal nuclei; PDGF α , platelet-derived growth factor alpha polypeptide; PDGF α , platelet-derived growth factor receptor; POLR2A, polymerase (RNA) II polypeptide A; RBfox3, RNA binding protein fox-1 homolog 3

Fig. 2 PH20 expression in the developing brain. qPCR analysis of PH20 expression in **a** primary cell culture from mouse and human brain cells. **b** PCR analysis of PH20 expression in the mouse cortex and corpus callosum of C57Bl/6, NU/NU, and SCID mice. Adult testis samples were used as positive control. Actb, beta-actin; bp, base pairs; G3PDH, glyceraldehyde 3-phosphate dehydrogenase; PCR, polymerase chain reaction; qPCR, quantitative polymerase chain reaction; SCID, severe combined immunodeficient mice



Prediction of rHuPH20 Affinity for HLA

To assess rHuPH20 peptide affinity for HLA, the rHuPH20 amino acid sequence was evaluated *in silico* against a panel of eight common Class II alleles, which together represent more than 95% of the human population. A total of 184 hits were identified in 3512 assessments, yielding an overall EpiMatrix Protein Score of -3.9. This score was within the neutral range and predicted relatively weak immunogenic potential for rHuPH20 with respect to T cell epitopes.

The 184 hits were further analyzed for the presence of known 9-mer T cell epitope clusters, which predict reactivity to >4 different HLA alleles. A total of nine clusters with immunogenic potential were identified (Table I). Collectively, these nine clusters contained 63% (116/184) of the EpiMatrix hits identified in the rHuPH20 protein while encompassing just 24% (107/439) of the 9-mer frames analyzed. Putative T cell epitope clusters identified within the rHuPH20 were screened for the presence of previously discovered T cell epitopes and major histocompatibility

Table I Potential T Cell Epitope Clusters in rHuPH20

Input sequence	Cluster address	Cluster sequence	EpiMatrix score	EpiBars? (#)
rHuPH20	11–25	NVPFLWAWNAPSEFC	15.10	Yes (1)
rHuPH20	34–51	DMSLFSFIGSPRINATGQ	18.62	Yes (1)
rHuPH20	125–148	PKDVYKNRSIELVQQQNVQLSLTE	32.72	Yes (3)
rHuPH20	166–185	VETIKLGKLLRPNHLWGYYL	11.55	No
rHuPH20	213–229	DLSWLWNESTALYPSIY	15.54	Yes (1)
rHuPH20	238–258	AATLYVRNRVREAIRVSKIPD	20.18	Yes (1)
rHuPH20	298–321	ASGIVIWGTLSIMRSMKSCLLLDN	44.88	Yes (4)
rHuPH20	327–345	LNPYIINVTLAAKMCSQVL	29.19	Yes (2)
rHuPH20	354–374	RKNWNSSDYHLHLPDNFAIQL	13.81	Yes (2)

EpiBars, single 9-mer amino acid sequence predictive to be reactive to >4 different human leukocytes alleles

rHuPH20, recombinant human hyaluronidase PH20

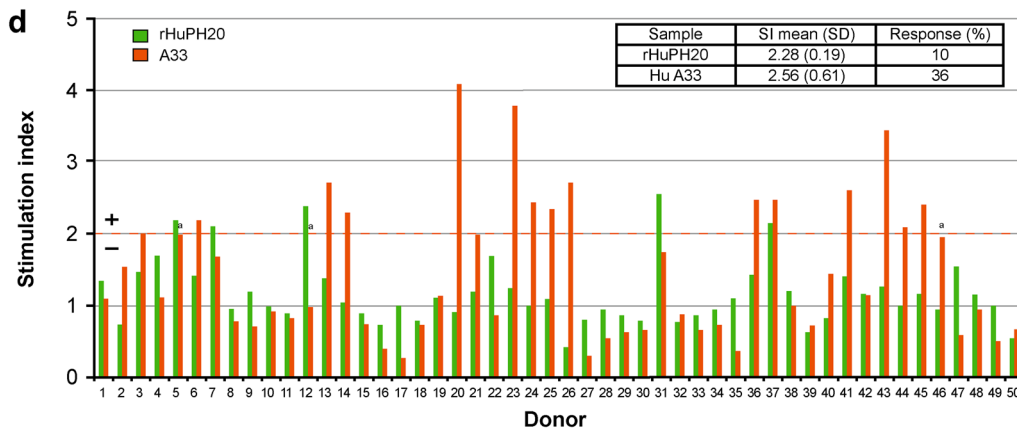
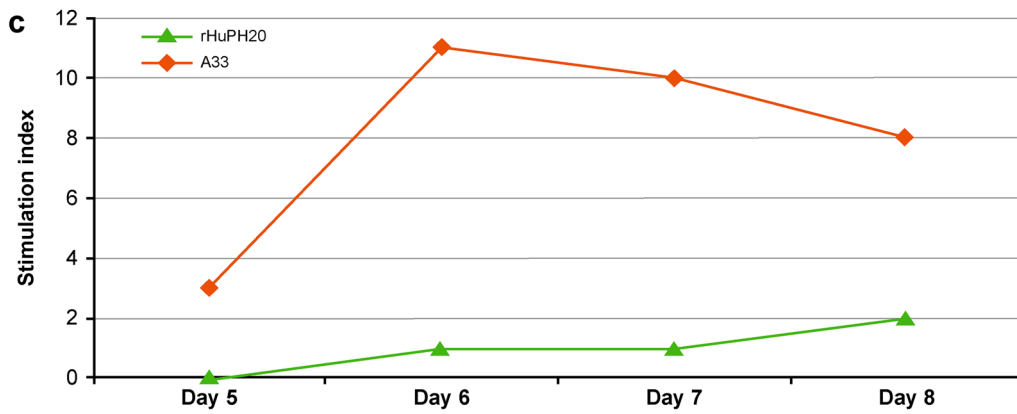
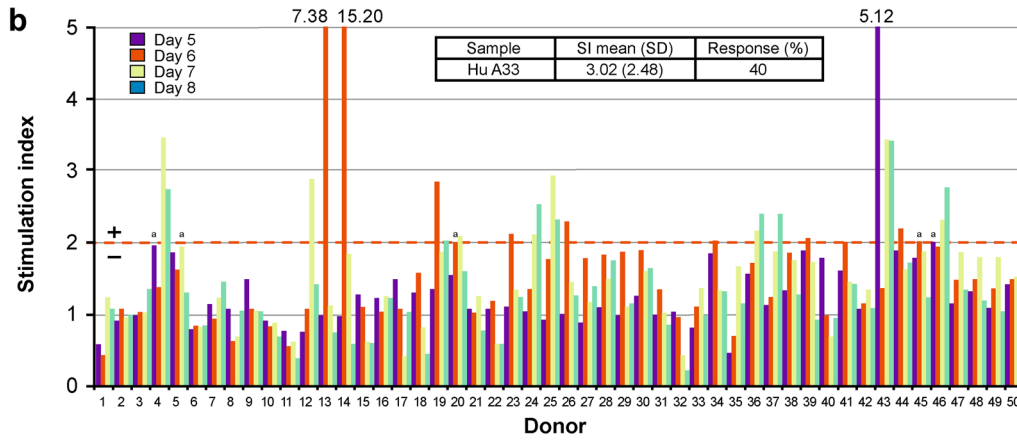
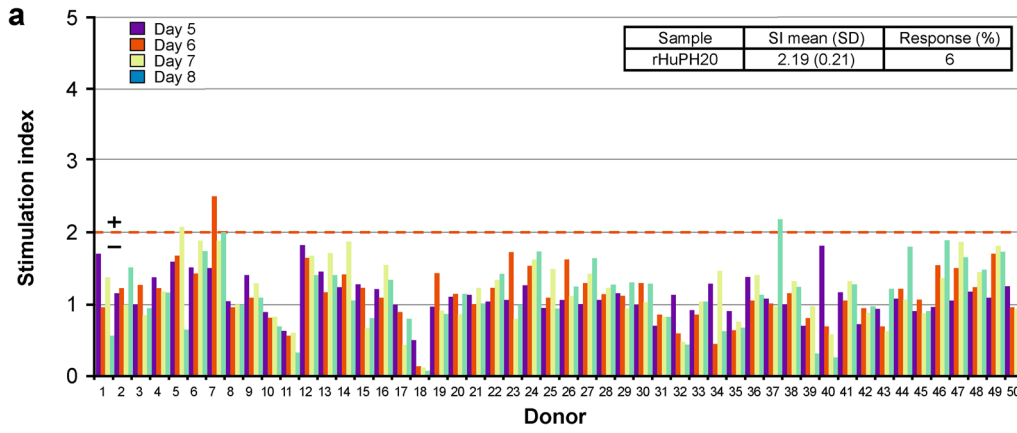


Fig. 3 T cell proliferation responses to **a** full length rHuPH20 and **b** humanized A33 positive control in PBMCs from 50 donors. **c** Number of positive T cell proliferation responses at days 5, 6, 7, and 8. **d** IL-2 responses to full length rHuPH20 and A33 positive control. Hu A33, humanized A33; IL-2, interleukin 2; PBMC, primary blood mononuclear cell; rHuPH20, recombinant human hyaluronidase PH20; SD, standard deviation; SI, stimulation index. ^aIndicates borderline responses ($P < 0.05$; $SI \geq 1.90$)

complex ligands. Of the nine clusters, only one (rHuPH20 125–148) was found to be homologous to HLA-DR1.

CD4+ T Cell Stimulation by rHuPH20

CD4+ T cell activation by rHuPH20 was assessed in PBMCs from healthy donors using T cell proliferation and IL-2 secretion assays. In the CD4+ T cell proliferation assay, the frequency of positive T cell proliferation responses was low. Positive T cell responses were defined by donors that produced a significant ($P < 0.05$) response with a stimulation index (SI) ≥ 2.00 . Full length rHuPH20 induced proliferation responses (mean SI 2.19 ± 0.21) in 6% of the PBMC cohort (Fig. 3a) compared with 40% in the humanized A33 control (Fig. 3b) with maximal T cell proliferation on day 5 (Fig. 3c). Similarly, IL-2 secretion (mean SI 2.28 ± 0.19) by CD4+ T cells following stimulation with full length rHuPH20 was observed in 10% of the PBMC cohort compared with 36% in the humanized A33 control (Fig. 3d).

The immunogenic potential of rHuPH20 was mapped by analysis of PBMC responses to five overlapping 15-mer peptides from rHuPH20. None of the peptides tested induced T cell proliferation in the study cohort above background threshold (SI ≥ 2.00 , $P < 0.05$; Fig. 4).

Prediction of Linear B Cell Epitopes in rHuPH20

The risk for rHuPH20-reactive antibodies to cross-react with B cells was assessed by analysis of a linear sequence of rHuPH20 and a 3D structure model for homology to known linear B cell epitopes. Based on consensus prediction, 15 potential antigenic epitopes were identified for rHuPH20. The highest sequence homology between the predicted epitopes in rHuPH20 and HYAL1 or HYAL2 was 54.5% (Table II).

Mapping of Linear B Cell Epitopes in rHuPH20

To map potential linear B cell epitopes in rHuPH20, the binding of three antibody preparations against rHuPH20 was analyzed on a rHuPH20 peptide array (Table III). The rHuPH20-reactive mouse 3E8 monoclonal IgG1 antibody recognized a single unique peptide on the array (peptide 28, amino acids from 136 to 150: LVQQQNVQLSLTEAT), and the rHuPH20-reactive rabbit polyclonal antibody bound 32

of 88 peptides in the array, corresponding to eight distinct sequence stretches. In contrast, the rHuPH20-reactive human IgG antibodies did not bind to the rHuPH20 peptide array (Table III).

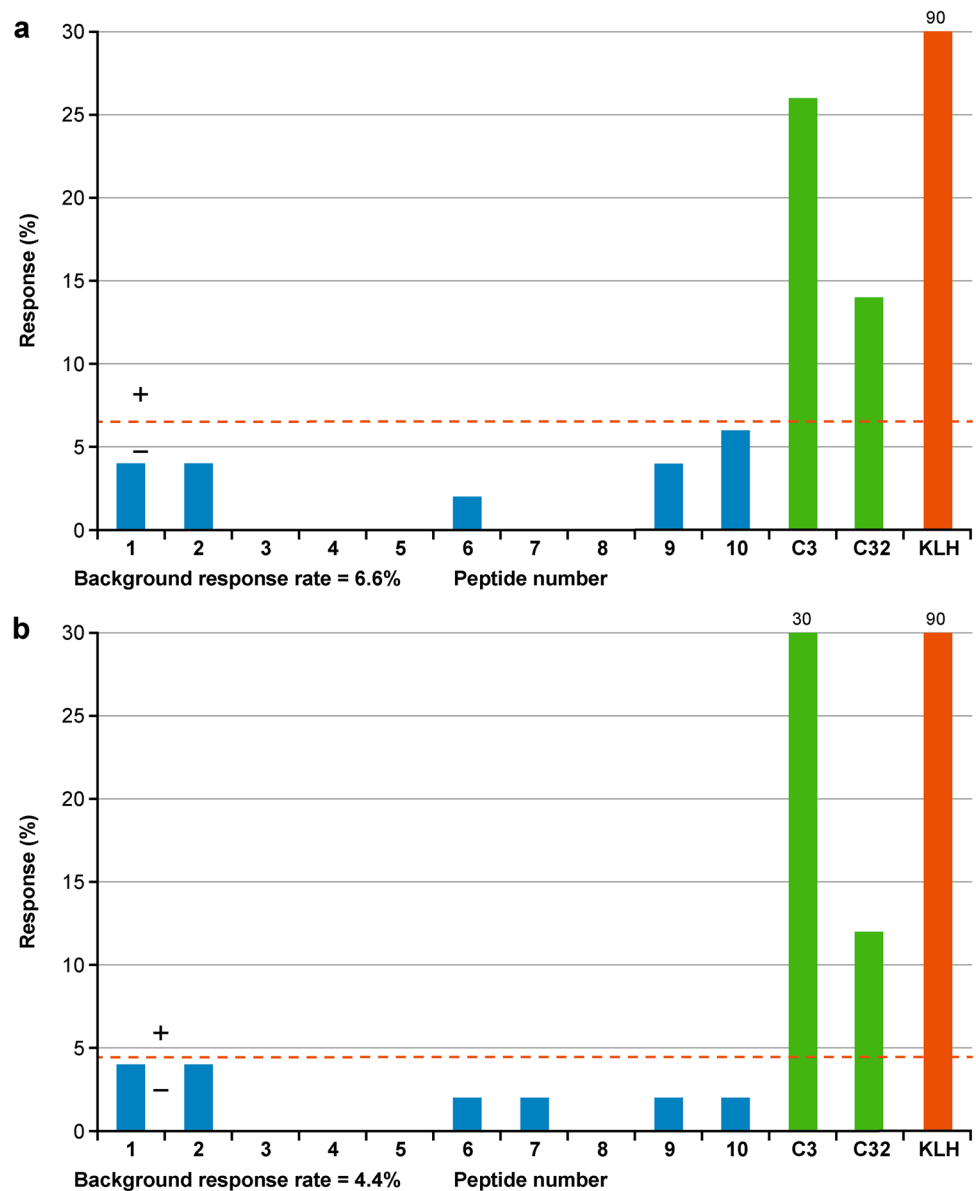
rHuPH20 Immunogenicity Findings from Clinical Trials

We collected data from clinical trials where rHuPH20 was co-administered with SC insulin/insulin analogs, trastuzumab (alone and in combination with pertuzumab), rituximab, human IgG, C1 esterase inhibitor, bococizumab, crenezumab, and daratumumab. The clinical immunogenicity of rHuPH20 was first assessed, in each trial, by the presence of anti-rHuPH20-binding antibodies using a validated bridging electrochemiluminescence immunoassay for binding antibodies. A modified hyaluronidase activity assay was used to assess the presence of neutralizing antibodies in anti-rHuPH20-positive antibody samples (21).

Among individual trials, the incidence of rHuPH20-reactive antibodies ranged from 0.9 to 44.7%, depending on the trial (Table IV). In cases where a high incidence of rHuPH20-reactive antibodies was observed, the result may be driven by the specific patient population and/or co-administered therapeutic. It is notable that by excluding a single clinical study that assessed co-administration of C1 esterase inhibitor with rHuPH20 (rHuPH20-reactive antibodies incidence of 44.7%) (37), this range is reduced to 0.9–18.9%. C1 esterase inhibitor is a human plasma-derived product that has low specific purity (69.6–89.5% of the protein of interest) (38) and it is possible the process-related impurities of human origin co-delivered with rHuPH20 in this setting enhanced the rHuPH20-reactive antibody response. Additionally, the data were obtained from only 47 subjects (37), which could affect the anti-drug antibody incidence. No neutralizing antibodies were detected in any subject from this study (37). Among trials that co-administered different monoclonal antibodies (daratumumab, rituximab, trastuzumab, crenezumab, bococizumab, and combination pertuzumab and trastuzumab), the incidence of treatment-emergent antibodies ranged from 0.9 to 18.9%, and in the trial that administered rHuPH20 sequentially with human immunoglobulin, the incidence rate was 18.1% (Table IV).

The cumulative incidence of treatment emergent rHuPH20-reactive antibodies in all clinical trials was 8.8% (233/2,643) (Table IV). Neutralizing antibodies were assessed in antibody-positive subjects. Across all studies, one patient from a completed study developed confirmed positive neutralizing antibodies, resulting in an overall incidence of 0.04% (1/2,643) in individuals exposed to rHuPH20. No clinical signs or symptoms have been associated with positive rHuPH20 antibody titers including neutralizing antibodies in clinical trials with rHuPH20.

Fig. 4 **a** Non adjusted and **b** adjusted response (removal of maximum and minimum CPM values to ensure low intra-assay variability) of peripheral blood mononuclear cells from healthy donors to rHuPH20 peptides in a T cell proliferation assay. Red line indicates the threshold for positive T cell proliferation responses ($SI \geq 2.00$, $P < 0.05$, including borderline responses $SI \geq 1.90$, $P < 0.05$). C3, Epstein Barr Virus nuclear antigen derived epitope; C32, influenza virus hemagglutinin derived epitope; CPM, counts per minute; KLH, Keyhole limpet hemocyanin; rHuPH20, recombinant human hyaluronidase PH20; SI, stimulation index



Discussion

Understanding tissue expression of hyaluronidase PH20 is important for evaluating the immunogenicity risk of rHuPH20. Due to the high homology of rHuPH20 to human hyaluronidase PH20 and with some homology to other human hyaluronidases (22), there is concern that rHuPH20-reactive antibodies could bind endogenous hyaluronidase PH20 (with or without neutralization), induce an allergic response, or attenuate local enzymatic activity at the SC injection site. We assessed tissue expression of hyaluronidases in a variety of adult and fetal human tissues and found that hyaluronidase PH20 expression is limited to the testes in human adults. The absence of hyaluronidase PH20 expression in human

adult brain tissue and cells of neuronal origin was in agreement with a directed query of the Allen Brain Atlas transcriptome database (36). Furthermore, hyaluronidase PH20 expression was not detected in primary neuronal cell cultures from humans or mice (27). Orthogonal assessments of PH20 expression including immunohistochemistry were evaluated and also demonstrated high levels of expression in the testes (39). Our findings, combined with published clinical data, indicate a low immunogenicity risk of SC rHuPH20. Additionally, we found low or undetectable hyaluronidase PH20 expression in all tissues other than the adult testes.

In silico and *in vitro* analysis of rHuPH20 revealed a low risk of immunogenicity. Being partially isolated from the body by the blood–testes barrier, sperm-derived proteins such as

Table II Predicted B Cell Epitopes in rHuPH20 and Relative Homology to HYAL1 and HYAL2 Sequence

Rank of rHuPH20 epitope	Residues (this refers to the rHuPH20 amino acid sequence)	Sequence	Match to consensus
1	371–387	AIQLEKGGKFTVRGKPT	6/17 (35%)
2	192–200	HHYKKPGY N	4/9 (44%)
3	355–362	KNW Δ SSDY	1/8 (12.5%)
4	44–51	PR I ATGQ	3/8 (37.5%)
6	66–77	YIDSITGVTVN	6/11 (54.5%)
7	256–262	IPDAKSP	1/7 (14.3%)
8	2–13	NFRAPPVIPNVP	6/12 (50%)
9	272–282	VFTDQVLKFLS	5/11 (45%)
10	305–312	GTLSIMRS	3/8 (37.5%)
11	97–106	TFYMPVDNLG	4/10 (40%)
12	140–145	QNVQLS	1/6 (16.7%)
13	27–37	GKFDEPLDMSL	4/11 (36.4%)
14	409–417	KEKADV KDT	0
15	437–443	PMET E EP	1/7 (14.3%)

N-linked glycosylation sites are indicated in italics, O-linked glycosylation sites are indicated in bold
HYAL1, hyaluronidase 1; *HYAL2*, hyaluronidase 2; *rHuPH20*, recombinant human hyaluronidase PH20

Table III rHuPH20-Reactive Antibodies Binding to the rHuPH20 Peptide Array

rHuPH20-reactive antibody	Peptide/sequence
Monoclonal mouse IgG1	LVQQQNVQLSLTEAT
Polyclonal rabbit IgG	LNFRAPPVIPNVPFL EPLDMSLFSFIGSPR NGGIPQKISLQDHLDKAKKDITFYMPVDNLGMAVIDWEEWRPTWARNWPKKD- VYKNRSIELVQQQNVQLS NVQLSLTEATEKAKQ LGKLLRPNHLWGYYLFPDCY VEIKRNDLDSWLWNE NWNSSDYLHLNPDNFAIQLEKGGKFTVRGKPTLEDLEQFSEKFCYSCYSTLSCKE DTDAVDVCIADGVCIDAFKPPMETEEPQIFY
Polyclonal human IgG	None

IgG, immunoglobulin G; *IgG1*, immunoglobulin G1; *rHuPH20*, recombinant human hyaluronidase PH20

hyaluronidase PH20 may potentially induce immunogenicity when introduced outside these immune privileged sites. The immunogenic potential of sperm and sperm-derived proteins has been reported in mice, rats, guinea pigs (40, 41), macaques (42), and sheep (31). Although rHuPH20 enzymatic activity in the SC space declines rapidly following administration (14, 43), rHuPH20 may be taken up by antigen presenting cells by binding HLA to stimulate T cell-directed immune responses (44).

Analysis of the rHuPH20 sequence revealed only one cluster with homology to HLA-DR1. These findings were corroborated *in vitro*, whereby rHuPH20 induced T cell activation in 6–10% of PBMCs from 50 healthy donors. Taken together, these data suggest that rHuPH20 has low

immunogenicity potential with respect to CD4+ T cell-induced responses.

rHuPH20-reactive antibodies could potentially cross-react with B cell epitopes in regions of homology to HYAL1, HYAL2, and HYAL3. However, 15 epitopes in the rHuPH20 sequence had the potential to interact with B cells, none of the rHuPH20 peptides interacted with anti-rHuPH20 human IgG polyclonal antibodies on the array, suggesting low potential for B cell epitope cross-reactivity. These findings agree with clinical trials reporting no cross-reactivity of rHuPH20-reactive antibodies to HYAL1 and HYAL2 (21). The lack of reactivity of anti-rHuPH20 antibodies to these hyaluronidase family members is of note, as HYAL1 and HYAL2 have broad expression patterns, are involved

Table IV Incidence of rHuPH20-Reactive Antibodies from SC Administration in Clinical Trials

Trial / sponsor	Co-administered therapeutic	Indication	Incidence of treatment-induced/enhanced rHuPH20-reactive antibodies in patients receiving rHuPH20 n/N (%)	Reference
117–203 / Halozyme	Insulin	Type I diabetes mellitus	1/40 (2.5)	(21)
117–205 / Halozyme	Insulin analog	Type I diabetes mellitus	5/113 (4.4)	(21)
117–206 / Halozyme	Insulin analog	Type II diabetes mellitus	2/116 (1.7)	(21)
117–403 / Halozyme	Continuous SC insulin infusion	Type I diabetes mellitus	24/335 (7.2)	(21)
HannaH / Roche ^a	Trastuzumab	HER-positive early breast cancer	36/290 (12.4)	(21)
SparkThera / Roche	Rituximab	Follicular lymphoma	6/185 (3.2)	(21)
SAWYER / Roche	Rituximab	Chronic lymphocytic leukemia	6/96 (6.3)	(21)
SABRINA / Roche	Rituximab	Follicular lymphoma	17/185 (9.2)	(21)
160603-902 / Baxter (Takeda)	Human IgG/HyQvia	Primary immunodeficiency/adult and pediatric	15/83 (18.1)	(21, 33)
NCT01756157 / Viropharma ^b	Human plasma-derived C1 inhibitor	Hereditary angioedema C1 inhibitor deficiency	21/47 (44.7)	(37)
NCT02667223 / Pfizer	Bococizumab	Hypercholesterolemia	4/45 (8.9)	(52)
NCT02519452 / Janssen	Daratumumab	Multiple myeloma	10/78 (12.8)	(24, 55)
COLUMBA / Janssen	Daratumumab	Multiple myeloma	19/255 (7.5)	(5)
PLEIADES / Janssen	Daratumumab	Multiple myeloma	16/192 (8.3)	(5)
MMY1004 / Janssen	Daratumumab	Multiple myeloma	21/111 (18.9)	N/A
FeDeriCa / Roche	Pertuzumab and trastuzumab	HER2-positive early breast cancer	2/225 (0.9)	(49)
GP40201 / Roche	Crenezumab	Autosomal-dominant Alzheimer's disease	1/36 (2.8)	(56)
ANDROMEDA / Janssen	Daratumumab	Light-chain amyloidosis	27/211 (12.8)	(54)
		Cumulative incidence n/N (%)	233/2643 (8.8)	

^aIncidence reported over the first 2 years of the HannaH study (21); in patients with a median follow-up of >5 years in the same study, the incidence was 21% (57); ^bAmong patients who developed rHuPH20-reactive antibodies, there was no increase in the incidence or severity of AEs and antibody titers decreased over time even during continued treatment

AE, adverse event; HER2, human epidermal growth factor receptor 2; IgG, immunoglobulin G; IgG1, immunoglobulin G1; rHuPH20, recombinant human hyaluronidase PH20; SC, subcutaneous

in somatic hyaluronan metabolism (45, 46), and deficiencies of each of these enzymes are associated with disease phenotypes (47).

Use of time course T cell assays for the assessment of immunogenic potential has its limitations. Although there was a good correlation between IL-2 production and proliferation after T cell activation, the percent of positive cells between these two markers of cell proliferation differed. These differences may be a result of transient proliferation responses missed in cultures before day 5, limited proliferation of specific T cell subsets, or the detection of both early and late responses in the IL-2 assay. Another limitation is the 3D model utilized in our prediction of B cell epitopes and which formed the basis for the peptide design. This model was based on the crystal structure of human HYAL1 using amino acids 2–403 of rHuPH20, rather than on rHuPH20 itself. However, as rHuPH20 shares 38% sequence identity

with HYAL1 (22), the modeled structure provides a reasonable representation of the rHuPH20 structure. Additionally, four of the 15 predicted B cell epitopes in rHuPH20 had glycosylation sites, which may have affected rankings if considered.

In clinical studies, in either rHuPH20 treatment-naïve patients or in healthy volunteers, 3–13% of subjects had detectable rHuPH20-reactive antibodies at baseline (21, 23, 24). The immunogenicity profile of rHuPH20 has been assessed in more than 20 clinical studies to date, including studies of rHuPH20 subcutaneously co-administered with human blood-derived polyclonal immunoglobulin (21), human insulin/insulin analogs (21, 48), human blood-derived C1 esterase inhibitor (37), trastuzumab (21, 49, 50), pertuzumab (49), rituximab (21, 51), bococizumab (52), daratumumab (24, 53–55), and crenezumab (56). Across trials, rHuPH20-reactive antibodies were detected in 0.9–44.7% of

patients treated with rHuPH20 (0.9–18.9% of patients treated with monoclonal antibodies; 18.1% of patients treated with human immunoglobulin; 44.7% of patients treated with C1 esterase) (21, 24, 37, 49, 51, 54–58). There was no reported association between rHuPH20-reactive antibodies and adverse events and where reported, anti-rHuPH20 antibodies did not appear to affect pharmacokinetic/exposure of the therapeutic molecule (5, 59). rHuPH20-neutralizing antibody activity has been confirmed in only one patient exposed to rHuPH20 from >20 clinical studies (>2500 subjects) to date, indicating low neutralization potential (<0.1% of exposed individuals) (21, 60). In addition, no allergic reactions to rHuPH20 were reported in a study evaluating sensitivity to a single dose of intradermally administered rHuPH20 in 100 healthy volunteers (61). The incidence of antibodies reactive to the therapeutic co-administered with rHuPH20 is similar regardless of administration route, with no particular trend for SC delivery (i.e., co-administration with rHuPH20) being more immunogenic than intravenous delivery (without rHuPH20) (5, 49, 57, 60, 62–66). Extensive clinical experience demonstrated that rHuPH20 is generally well tolerated when combined with a range of co-administered therapeutic agents, across diverse patient groups and over a long duration.

The mechanism of action of the biotherapeutics co-administered with rHuPH20 across the clinical trials may have impacted the incidence of anti-drug antibodies. Molecules that are immunomodulatory in nature, such as the anti-CD20 molecule rituximab, which causes B cell lysis (62), could potentially reduce anti-rHuPH20 antibody titers and/or responses. Attributes of the specific patient populations could also affect the anti-drug antibody incidence. Anticancer therapies are typically administered to immunosuppressed patients who may have diminished anti-drug antibody formation relative to fully immune competent patient populations (67). Similarly, human IgG is administered sequentially with rHuPH20 to patients with primary immune deficiencies who may have an impaired or absent ability to generate competent antibody responses (e.g., as seen in patients with severe combined immunodeficiency) (33, 68).

Conclusions

Using a variety of tissue samples and state of the art techniques to measure gene expression, we confirmed that hyaluronidase PH20 expression is localized primarily in adult human testes, with no expression detected in other tissues including the cartilage, kidney, and brain. *In silico* and *in vitro* analyses suggest a low immunogenicity potential of rHuPH20 with respect to CD4+ T cell activation and B cell cross-reactivity. Overall, across trials, 0.9–44.7% of patients

treated with rHuPH20 had treatment-emergent rHuPH20-reactive antibodies and the development of rHuPH20-reactive antibodies has not been associated with adverse events. Taken together, our findings combined with this wealth of clinical data and experience, indicate that the immunogenicity risk of SC rHuPH20 is low.

Supplementary Information The online version contains supplementary material available at <https://doi.org/10.1208/s12248-022-00757-3>.

Acknowledgements The authors would like to thank Gregory I. Frost for his valuable contribution to this work, Stephen Knowles (Halozyme Therapeutics, Inc., San Diego, CA, USA), David Citerone, and Ivo Nnane (Janssen R & D, LLC, Spring House, PA, USA) for their insightful review of this manuscript, EpiVax and ProImmune for completing the *in silico* and *in vitro* risk assessments, and Beckman Coulter Genomics for conducting the RNA-Seq analysis. Medical writing support, including assisting authors with the development of the outline and initial draft, and incorporation of comments, was provided by Jennifer Brewins, PhD, and Miriam Cohen, PhD; editorial support was provided by Michelle Seddon, all of Paragon, Knutsford, UK, supported by Halozyme Therapeutics, Inc. Halozyme Therapeutics, Inc. follows all current policies established by the International Committee of Medical Journal Editors and Good Publication Practice guidelines (link). The sponsor was involved in the study design and collection, analysis, and interpretation of data, as well as data checking of information provided in the manuscript. However, ultimate responsibility for opinions, conclusions, and data interpretation lies with the authors.

Author Contribution MAP, BJS, RDP, MCJ, DCM, and MJL were responsible for the conception and design of the study. Acquisition of data was carried out by MAP, BJS, RDP, MCJ, YW, and DWK. Analysis or interpretation of data was carried out by MAP, BJS, RDP, MCJ, YW, DCM, and MJL. All authors contributed to drafting the work or revising it critically for important intellectual content.

Funding The study was supported by Halozyme Therapeutics, Inc.

Data Availability Halozyme Therapeutics, Inc., follows policies established by the International Committee of Medical Journal Editors. Halozyme Therapeutics, Inc. holds the data for studies that were conducted by the company. Additional information about the studies and/or datasets can be obtained by contacting Halozyme Therapeutics, Inc.: 11388 Sorrento Valley Road, San Diego, CA 92121, USA; phone: +1.858.794.8889; email: publications@halozyme.com.

Declarations

Ethics Approval All procedures performed in studies involving human participants were in accordance with the ethical standards of the institutional and/or national research committee, and with the 1964 Helsinki Declaration and its later amendments or comparable ethical standards.

Competing Interests DWK, MAP, MJL, and YW are employees of Halozyme Therapeutics, Inc. BJS, DCM, MCJ, and RDP were employees of Halozyme Therapeutics, Inc., at the time of the study. DCM, DWK, MAP, MJL, and YW are shareholders of Halozyme Therapeutics, Inc. MJ and RP declare no competing interests.

Open Access This article is licensed under a Creative Commons Attribution 4.0 International License, which permits use, sharing, adaptation, distribution and reproduction in any medium or format, as long as you give appropriate credit to the original author(s) and the source, provide a link to the Creative Commons licence, and indicate if changes

were made. The images or other third party material in this article are included in the article's Creative Commons licence, unless indicated otherwise in a credit line to the material. If material is not included in the article's Creative Commons licence and your intended use is not permitted by statutory regulation or exceeds the permitted use, you will need to obtain permission directly from the copyright holder. To view a copy of this licence, visit <http://creativecommons.org/licenses/by/4.0/>.

References

- Stern R. Devising a pathway for hyaluronan catabolism: are we there yet? *Glycobiology*. 2003;13:105R–15R.
- Cowman MK, Lee HG, Schwertfeger KL, McCarthy JB, Turley EA. The content and size of hyaluronan in biological fluids and tissues. *Front Immunol*. 2015;6:261.
- Toole BP. Hyaluronan: from extracellular glue to pericellular cue. *Nat Rev Cancer*. 2004;4:528–39.
- Csoka AB, Frost GI, Stern R. The six hyaluronidase-like genes in the human and mouse genomes. *Matrix Biol*. 2001;20:499–508.
- Janssen Biotech Inc. DARZALEX FASPRO™ prescribing information for subcutaneous use. 2022. <https://www.janssenlabels.com/package-insert/product-monograph/prescribing-information/DARZALEX+Faspro-pi.pdf>. Accessed September 13, 2022.
- Evans EA, Zhang H, Martin-DeLeon PA. SPAM1 (PH-20) protein and mRNA expression in the epididymides of humans and macaques: utilizing laser microdissection/RT-PCR. *Reprod Biol Endocrinol*. 2003;1:54.
- Deng X, He Y, Martin-DeLeon PA. Mouse Spam1 (PH-20): evidence for its expression in the epididymis and for a new category of spermatogenic-expressed genes. *J Androl*. 2000;21:822–32.
- El Hajjaji H, Cole AA, Manicourt DH. Chondrocytes, synovio-cytes and dermal fibroblasts all express PH-20, a hyaluronidase active at neutral pH. *Arthritis Res Ther*. 2005;7:R756–68.
- Beech DJ, Madan AK, Deng N. Expression of PH-20 in normal and neoplastic breast tissue. *J Surg Res*. 2002;103:203–7.
- Grigorieva A, Griffiths GS, Zhang H, Laverty G, Shao M, Taylor L, et al. Expression of SPAM1 (PH-20) in the murine kidney is not accompanied by hyaluronidase activity: evidence for potential roles in fluid and water reabsorption. *Kidney Blood Press Res*. 2007;30:145–55.
- Zhang H, Martin-DeLeon PA. Mouse Spam1 (PH-20) is a multi-functional protein: evidence for its expression in the female reproductive tract. *Biol Reprod*. 2003;69:446–54.
- Sloane JA, Batt C, Ma Y, Harris ZM, Trapp B, Vartanian T. Hyaluronan blocks oligodendrocyte progenitor maturation and remyelination through TLR2. *Proc Natl Acad Sci USA*. 2010;107:11555–60.
- Preston M, Gong X, Su W, Matsumoto SG, Banine F, Winkler C, et al. Digestion products of the PH20 hyaluronidase inhibit remyelination. *Ann Neurol*. 2013;73:266–80.
- Bookbinder LH, Hofer A, Haller MF, Zepeda ML, Keller GA, Lim JE, et al. A recombinant human enzyme for enhanced interstitial transport of therapeutics. *J Control Release*. 2006;114:230–41.
- Halozyne Therapeutics Inc. HYLENEX recombinant prescribing information. 2016. <http://hylene.com/downloads/approved-uspi-1b1301feb2016.pdf>. Accessed June 7, 2022.
- Printz MA, Dychter SS, DeNoia EP, Harrigan R, Sugarman BJ, Zepeda M, et al. A phase I study to evaluate the safety, tolerability, pharmacokinetics, and pharmacodynamics of recombinant human hyaluronidase PH20 administered intravenously in healthy volunteers. *Curr Ther Res Clin Exp*. 2020;93:100604.
- Kuriakose A, Chirmule N, Nair P. Immunogenicity of biotherapeutics: causes and association with posttranslational modifications. *J Immunol Res*. 2016;2016:1298473.
- Li J, Yang C, Xia Y, Bertino A, Glaspy J, Roberts M, et al. Thrombocytopenia caused by the development of antibodies to thrombopoietin. *Blood*. 2001;98:3241–8.
- Lim LC. Acquired red cell aplasia in association with the use of recombinant erythropoietin in chronic renal failure. *Hematology*. 2005;10:255–9.
- Ragnhammar P, Wadhwa M. Neutralising antibodies to granulocyte-macrophage colony stimulating factor (GM-CSF) in carcinoma patients following GM-CSF combination therapy. *Med Oncol*. 1996;13:161–6.
- Rosengren S, Dychter SS, Printz MA, Huang L, Schiff RI, Schwarz HP, et al. Clinical immunogenicity of rHuPH20, a hyaluronidase enabling subcutaneous drug administration. *AAPS J*. 2015;17:1144–56.
- Stern R, Jedrzejewski MJ. Hyaluronidases: their genomics, structures, and mechanisms of action. *Chem Rev*. 2006;106:818–39.
- Rosengren S, Souratha J, Conway D, Muchmore DB, Sugarman BJ. Recombinant human PH20: baseline analysis of the reactive antibody prevalence in the general population using healthy subjects. *BioDrugs*. 2018;32:83–9.
- Usmani SZ, Nahi H, Mateos MV, van de Donk N, Chari A, Kaufman JL, et al. Subcutaneous delivery of daratumumab in relapsed or refractory multiple myeloma. *Blood*. 2019;134:668–77.
- Baba D, Kashiwabara S, Honda A, Yamagata K, Wu Q, Ikawa M, et al. Mouse sperm lacking cell surface hyaluronidase PH-20 can pass through the layer of cumulus cells and fertilize the egg. *J Biol Chem*. 2002;277:30310–4.
- Park S, Kim YH, Jeong PS, Park C, Lee JW, Kim JS, et al. SPAM1/HYAL5 double deficiency in male mice leads to severe male subfertility caused by a cumulus-oocyte complex penetration defect. *FASEB J*. 2019;33:14440–9.
- Marella M, Ouyang J, Zombeck J, Zhao C, Huang L, Connor RJ, et al. PH20 is not expressed in murine CNS and oligodendrocyte precursor cells. *Ann Clin Transl Neurol*. 2017;4:191–211.
- Cherr GN, Yudin AI, Overstreet JW. The dual functions of GPI-anchored PH-20: hyaluronidase and intracellular signaling. *Matrix Biol*. 2001;20:515–25.
- Hardy CM, Clydesdale G, Mobbs KJ, Pekin J, Lloyd ML, Sweet C, et al. Assessment of contraceptive vaccines based on recombinant mouse sperm protein PH20. *Reproduction*. 2004;127:325–34.
- Pomeroy M, Jones RC, Holland MK, Blake AE, Beagley KW. Restricted entry of IgG into male and female rabbit reproductive ducts following immunization with recombinant rabbit PH-20. *Am J Reprod Immunol*. 2002;47:174–82.
- Morton DB, McAnulty PA. The effect on fertility of immunizing female sheep with ram sperm acrosin and hyaluronidase. *J Reprod Immunol*. 1979;1:61–73.
- Bertrand P, Girard N, Duval C, d'Anjou J, Chauzy C, Menard JF, et al. Increased hyaluronidase levels in breast tumor metastases. *Int J Cancer*. 1997;73:327–31.
- Baxalta US Inc. HYQVIA prescribing information for HyQvia: immune globulin infusion 10% (human) with recombinant human hyaluronidase. 2021. https://www.shirecontent.com/PI/PDFs/HYQVIA_USA_ENG.pdf. Accessed September 13, 2022.
- Li N, Wang T, Han D. Structural, cellular and molecular aspects of immune privilege in the testis. *Front Immunol*. 2012;3:152.
- Alexander NJ. Natural and induced immunological infertility. *Curr Opin Immunol*. 1989;1:1125–30.
- Hawrylycz MJ, Lein ES, Guillozet-Bongaarts AL, Shen EH, Ng L, Miller JA, et al. An anatomically comprehensive atlas of the adult human brain transcriptome. *Nature*. 2012;489:391–9.

37. Riedl MA, Lumry WR, Li HH, Banerji A, Bernstein JA, Ba M, et al. Subcutaneous administration of human C1 inhibitor with recombinant human hyaluronidase in patients with hereditary angioedema. *Allergy Asthma Proc.* 2016;37:489–500.
38. Feussner A, Kalina U, Hofmann P, Machnig T, Henkel G. Biochemical comparison of four commercially available C1 esterase inhibitor concentrates for treatment of hereditary angioedema. *Transfusion.* 2014;54:2566–73.
39. Baxter Healthcare Corporation, Baxter BioScience. HyQvia: immune globulin infusion 10% (human) with recombinant human hyaluronidase, Blood Products Advisory Committee Briefing Book. 2014. <https://wayback.archive-it.org/7993/20170113014523/http://www.fda.gov/downloads/AdvisoryCommittees/CommitteesMeetingMaterials/BloodVaccinesandOtherBiologics/BloodProductsAdvisoryCommittee/UCM407013.pdf>. September 13, 2022.
40. Kohno S, Munoz JA, Williams TM, Teuscher C, Bernard CC, Tung KS. Immunopathology of murine experimental allergic orchitis. *J Immunol.* 1983;130:2675–82.
41. Teuscher C, Wild GC, Tung KS. Immunochemical analysis of guinea pig sperm autoantigens. *Biol Reprod.* 1982;26:218–29.
42. Rana R, Jagadish N, Garg M, Mishra D, Dahiya N, Chaurasiya D, et al. Immunogenicity study of recombinant human sperm-associated antigen 9 in bonnet macaque (*Macaca radiata*). *Hum Reprod.* 2006;21:2894–900.
43. Frost GI. Recombinant human hyaluronidase (rHuPH20): an enabling platform for subcutaneous drug and fluid administration. *Exp Opin Drug Deliv.* 2007;4:427–40.
44. Couture A, Garnier A, Docagne F, Boyer O, Vivien D, Le-Mauff B, et al. HLA-class II artificial antigen presenting cells in CD4(+) T cell-based immunotherapy. *Front Immunol.* 2019;10:1081.
45. Stern R. Hyaluronan catabolism: a new metabolic pathway. *Eur J Cell Biol.* 2004;83:317–25.
46. Erickson M, Stern R. Chain gangs: new aspects of hyaluronan metabolism. *Biochem Res Int.* 2012;2012:893947.
47. Triggs-Raine B, Natowicz MR. Biology of hyaluronan: insights from genetic disorders of hyaluronan metabolism. *World J Biol Chem.* 2015;6:110–20.
48. Vaughn DE, Muchmore DB. Use of recombinant human hyaluronidase to accelerate rapid insulin analogue absorption: experience with subcutaneous injection and continuous infusion. *Endocr Pract.* 2011;17:914–21.
49. Genentech Inc. PHESGO (pertuzumab, trastuzumab, and hyaluronidase-zzxf) injection, for subcutaneous use. 2020. https://www.gene.com/download/pdf/phesgo_prescribing.pdf. Accessed September 13, 2022.
50. Ismael G, Hegg R, Muehlbauer S, Heinzmann D, Lum B, Kim SB, et al. Subcutaneous versus intravenous administration of (neo) adjuvant trastuzumab in patients with HER2-positive, clinical stage I-III breast cancer (HannaH study): a phase 3, open-label, multicentre, randomised trial. *Lancet Oncol.* 2012;13:869–78.
51. Davies A, Merli F, Mihaljevic B, Mercadal S, Siritanaratkul N, Solal-Celigny P, et al. Efficacy and safety of subcutaneous rituximab versus intravenous rituximab for first-line treatment of follicular lymphoma (SABRINA): a randomised, open-label, phase 3 trial. *Lancet Haematol.* 2017;4:e272–e82.
52. Bass A, Plotka A, Mridha K, Sattler C, Kim AM, Plowchalk DR. Pharmacokinetics, pharmacodynamics, and safety of bococizumab, a monoclonal antibody against proprotein convertase subtilisin/kexin type 9, in healthy subjects when administered in co-mixture with recombinant human hyaluronidase: a phase 1 randomised trial. *Health Sci Rep.* 2018;1:e61.
53. Mateos MV, Nahi H, Legiec W, Grosicki S, Vorobyev V, Spicka I, et al. Subcutaneous versus intravenous daratumumab in patients with relapsed or refractory multiple myeloma (COLUMBA): a multicentre, open-label, non-inferiority, randomised, phase 3 trial. *Lancet Haematol.* 2020;7:e370–e80.
54. Luo MM, Zhu PP, Nnane I, Xiong Y, Merlini G, Comenzo RL, et al. Population pharmacokinetics and exposure-response modeling of daratumumab subcutaneous administration in patients with light-chain amyloidosis. *J Clin Pharmacol.* 2022;62:656–69.
55. San-Miguel J, Usmani SZ, Mateos MV, van de Donk N, Kaufman JL, Moreau P, et al. Subcutaneous daratumumab in patients with relapsed or refractory multiple myeloma: part 2 of the open-label, multicenter, dose-escalation phase 1b study (PAVO). *Haematologica.* 2021;106:1725–32.
56. Dolton MJ, Chesterman A, Moein A, Sink KM, Waitz A, Blondeau K, et al. Safety, tolerability, and pharmacokinetics of high-volume subcutaneous crenezumab, with and without recombinant human hyaluronidase in healthy volunteers. *Clin Pharmacol Ther.* 2021;110:1337–48.
57. Roche Products Ltd. HERCEPTIN HYLECTA™ prescribing information for subcutaneous use. 2019. https://www.accessdata.fda.gov/drugsatfda_docs/label/2019/761106s0001bl.pdf. Accessed September 13, 2022.
58. Usmani SZ, Mateos M-V, Nahi H, Grosicki S, Vorobyev VI, Spicka I, et al. Randomized, open-label, non-inferiority, phase 3 study of subcutaneous (SC) versus intravenous (IV) daratumumab (DARA) administration in patients with relapsed or refractory multiple myeloma: Columba update. *Blood.* 2019;134:1865.
59. Angelotti F, Capocchi R, Giannini D, Mazzarella O, Rocchi V, Migliorini P. Long-term efficacy, safety, and tolerability of recombinant human hyaluronidase-facilitated subcutaneous infusion of immunoglobulin (Ig) (fSCIG; HyQvia®) in immunodeficiency diseases: real-life data from a monocentric experience. *Clin Exp Med.* 2020;20:387–92.
60. Knowles SP, Printz MA, Kang DW, LaBarre MJ, Tannenbaum RP. Safety of recombinant human hyaluronidase PH20 for subcutaneous drug delivery. *Exp Opin Drug Deliv.* 2021;18:1673–85.
61. Yocum RC, Kennard D, Heiner LS. Assessment and implication of the allergic sensitivity to a single dose of recombinant human hyaluronidase injection: a double-blind, placebo-controlled clinical trial. *J Infus Nurs.* 2007;30:293–9.
62. Genentech Inc. Prescribing information RITUXAN HYCELA™ (rituximab and hyaluronidase human) injection, for subcutaneous use. 2021. https://www.gene.com/download/pdf/rituxan_hycela_prescribing.pdf. Accessed September 13, 2022.
63. Genentech Inc. PERJETA® (pertuzumab) injection, for intravenous use. 2021. https://www.gene.com/download/pdf/perjeta_prescribing.pdf. Accessed September 12, 2022.
64. Janssen Biotech Inc. Prescribing information. Darzalex (daratumumab) injection for intravenous use. 2022. <http://www.janssenlabels.com/package-insert/product-monograph/prescribing-information/DARZALEX-pi.pdf>. Accessed September 12, 2022.
65. Genentech Inc. HERCEPTIN® (trastuzumab), for intravenous use. 2021. https://www.gene.com/download/pdf/herceptin_prescribing.pdf. Accessed September 12, 2022.
66. Genentech Inc. RITUXAN® (rituximab) injection, for intravenous use. 2021. https://www.gene.com/download/pdf/rituxan_prescribing.pdf. Accessed September 12, 2022.
67. van Brummelen EMJ, Ros W, Wolbink G, Beijnen JH, Schellens JHM. Antidrug antibody formation in oncology: clinical relevance and challenges. *Oncologist.* 2016;21:1260–8.
68. Picard C, Bobby Gaspar H, Al-Herz W, Bousfiha A, Casanova JL, Chatila T, et al. International union of immunological societies: 2017 primary immunodeficiency diseases committee report on inborn errors of immunity. *J Clin Immunol.* 2018;38:96–128.

Publisher's Note Springer Nature remains neutral with regard to jurisdictional claims in published maps and institutional affiliations.

Supplementary Information

Supplementary Table I. Murine PH20 primer sets

Primer set	Forward primer	Reverse primer	Amplicon
PH20_124	5'-TGGGATGCTATGAGTTTAGC-3'	5'-CAAAGTGTTTGGCTGCACAT-3'	124 bp
PH20_440	5'-ATGGAAGGAACTTTACACCT-3'	5'-GCTAAACTCATAGCATCCCA-3'	440 bp
PH20_588	5'-TGGGATGCTATGAGTTTAGC-3'	5'-CCAAATTACTGAGGCCTGCA-3'	588 bp

bp, base pairs

Supplementary Table II. Sequences of full length rHuPH20 and overlapping peptides

Peptide	Sequence
Peptide 1	NHHYKKPGYNGSCFN
Peptide 3	YKKPGYNGSCFNVEI
Peptide 5	PGYNGSCFNVEIKRN
Peptide 7	NGSCFNVEIKRNDDL
Peptide 9	CFNVEIKRNDDLSWL
rHuPH20 (full length)	LNFRAPPVIPNVPFLWAWNAPSEFCLGKFDEPLDMSLFSFIGSPRINATGQGVTIFY VDRLGYYPYIDSITGVTVNGGIPQKISLQDHLKAKKDITFYMPVDNLGMAVIDWEE WRPTWARNWPKPKDVYKNRSIELVQQQNVQLSLTEATEKAKQEFEKAGKDFLVETI KLGKLLRPNHLWGYYLFPDCYNHHYKKPGYNGSCFNVEIKRNDDLSWLWNESTA LYPSIYLNTQQSPVAATLYVRNRVREAIRVSKIPDAKSPLPVFAYTRIVFTDQVLKFL SQDELVYTFGETVALGASGIVIWGTLSIMRSMKSCLLLDNYMETILNPYIINVTLAAK MCSQVLCQEQGVCIRKNWNSSDYHLNPDNFQAIQLEKGGKFTVRGKPTLEDLEQF SEKFYCSYSTLSCKEKADVKTDAVDVCIADGVCIDAFLKPPMETEEPQIFY

rHuPH20, recombinant human hyaluronidase PH20

Supplementary Table III. Control features printed along test peptides

Control featured printed alongside test peptides

Standard ProArray Ultra™ controls:

Mouse IgG (100, 50, 25, 12.5, 6.25 µg/mL)

Human IgG (100, 50, 25, 12.5, 6.25 µg/mL)

Human IgM (100 µg/mL)

Negative control features (no peptide)

Customer control:

rHuPH20 (100 µg/mL)

IgG, immunoglobulin G; IgM, immunoglobulin M; rHuPH20, recombinant human hyaluronidase PH20